Osteoarthritis and Cartilage 24 (2016) 1883–1889

Osteoarthritis and Cartilage

A novel method for assessing signal intensity within infrapatellar fat pad on MR images in patients with knee osteoarthritis

M. Lu † ‡ § [a], Z. Chen † || [a], W. Han †, Z. Zhu † §, X. Jin †, D.J. Hunter ¶, C. Ding † § ¶ *

† *Menzies Institute for Medical Research, University of Tasmania, Hobart, Tasmania, Australia*
‡ *Department of Orthopaedics, 1st Affiliated Hospital, Anhui Medical University, Hefei, Anhui, China*
§ *Arthritis Research Institute, 1st Affiliated Hospital, Anhui Medical University, Hefei, Anhui, China*
|| *School of Engineering, Southeast University, Nanjing, China*
¶ *Institute of Bone and Joint Research, Kolling Institute, University of Sydney; Rheumatology Department, Royal North Shore Hospital, Sydney, NSW, Australia*

ARTICLE INFO

Article history:
Received 8 November 2015
Accepted 11 June 2016

Keywords:
Osteoarthritis
Infrapatellar fat pad
High signal intensity
MR images

SUMMARY

Purpose: To assess reliability and validity of a semi-automated quantitative method to measure infrapatellar fat pad (IPFP) signal intensity in patients with knee osteoarthritis (OA).
Methods: Hundred patients with knee OA were selected. Sagittal planes of fat-saturated T2-weighted images obtained on 1.5-T magnetic resonance imaging (MRI) were utilized to assess IPFP signal intensity using MATLAB. Knee structural abnormalities including cartilage defects, bone marrow lesions (BML) and radiographic OA (ROA) were evaluated.
Clinical construct validity and concurrent validity were examined through describing associations of IPFP measurements with knee structural abnormalities and a semi-quantitative scoring method, respectively. The reliability was examined by calculating the intra- and inter-observer correlation coefficients.
Results: Significantly positive associations were found between standard deviation of IPFP signal intensity [sDev (IPFP)], clustering factor (H) and all knee structural abnormalities. The volume of high signal intensity regions [Volume (H)] and the ratio of Volume (H) to volume of whole IPFP [Percentage (H)] were positively associated with cartilage defects and ROA, but not with BMLs. The median value [Median (H)] and upper quartile value [UQ (H)] of high signal intensity were only significantly associated with quartiles of cartilage defect score. Significant correlations were found between all quantitative measurements and semi-quantitative scores (All $P < 0.001$). Intraclass and interclass correlation coefficients for these quantitative measures were high (>0.90).
Conclusions: A novel and efficient method to segment IPFP and calculate its signal intensity on T2-weighted MRI images is documented. This method is reproducible, and has concurrent and clinical construct validity, but its predictive validity needs to be examined by future longitudinal studies.

Introduction

Knee osteoarthritis (OA) is characterized by gradual loss of articular cartilage and formation of osteophytes[1]. Other joint tissues including synovium, menisci, ligaments, periarticular muscles and the joint capsule are also involved[2]. Infrapatellar fat pad (IPFP), which is an intracapsular and extrasynovial adipose structure in the knee joint, may play a key role in knee OA by modulating and influencing neighbouring tissues of the joint[3].

Magnetic resonance imaging (MRI) offers detailed insight into OA pathology and is useful for evaluating IPFP[4]. Both maximal area and volume of IPFP have been used to measure the quantity of IPFP on MRI in recent studies[5,6] which reported that IPFP size had a protective effect against knee symptomatic and structural changes[5]. Abnormal quality of IPFP has also been investigated by assessing IPFP signal intensity changes or Hoffa's synovitis on MRI, which was significantly associated with increased symptoms, incident radiographic OA (ROA), or abnormal changes in knee structures[7,8]. The abnormal quality was assessed semi-quantitatively using subjective scoring systems; however, the

* Address correspondence and reprint requests to: C. Ding, Private Bag 23, Hobart, Tasmania 7000, Australia. Tel: 61-3-62267730; Fax: 61-3-62267704.
E-mail address: Changhai.Ding@utas.edu.au (C. Ding).
[a] Ming Lu and Zhongshan Chen contributed equally.

http://dx.doi.org/10.1016/j.joca.2016.06.008
1063-4584/

automated quantitative measurements of the signal intensity changes, which can be more efficient and cost saving, are scarce and just under development[9].

The purpose of this study is to develop and validate a novel quantitative method of measuring signal intensity of IPFP through comparison with a semi-quantitative scoring system and describing their associations with knee structural abnormalities.

Materials and methods

Study sample

We used data from Vitamin D Effect on Osteoarthritis (VIDEO) study, a multicentre randomized, double-blind and placebo-controlled clinical trial for evaluating the effects of vitamin D supplementation on knee pain and structural changes in knee OA patients with low 25-hydroxy vitamin D [25(OH)D]. Inclusion criteria included symptomatic knee OA for at least 6 months assessed according to American College of Rheumatology (ACR) criteria for clinical knee OA[10], visual analogue scale (VAS) scores of more than 20 mm and serum 25 (OH)D levels between 12.5 nmol/L and 60 nmol/L. Exclusion criteria included grade 3 radiographic changes according to the Altman's atlas[11], severe knee pain on standing (more than 80 mm on a 100 mm VAS), contraindication to MRI, other forms for arthritis such as rheumatoid or psoriatic arthritis, severe renal impairment, and others[12]. For the current study, the first 100 participants from this randomized controlled clinical trial in Tasmania were selected as study participants for the MRI measurements of IPFP. Ethics approval has been received from The Tasmania Health and Human Medical Research Ethics Committee (reference member H1040). Informed written consent was obtained from all participants.

MRI protocol

MRI of the study knees was obtained on a non-contrast 1.5-T whole body MRI unit (Picker, Cleveland, OH, USA) using a commercial transmit-receive extremity coil. Sagittal planes of T2-weighted sequence were used. The parameters of the MRI sequence are as follows: a T2-weighted fat-saturated 3-D fast spin echo, flip angle 90°, repetition time 3067 ms, echo time 112 ms, field of view 16 cm/15 partitions, 228 × 256-pixel matrix; sagittal images were obtained at a partition thickness of 2 mm. There were around 45 MRI slices for the whole knee and around 15 slices that had IPFP and were used to analyse IPFP signal intensity.

Image analysis

Sagittal planes of fat-saturated T2-weighted images were selected using MATLAB (MATLAB 8.4, The MathWorks Inc., Natick, MA, United States). The reader manually chose a set of points in sequence near the outer contour of IPFP and created an initial lasso around IPFP. The initial lasso contracted inward and approximated to the boundary of IPFP automatically until the actual edge was approached [Fig. 1(a)].

This algorithm was well designed to segment IPFP semi-automatically. Compared with the traditional algorithm, the new one was based on an improved based-canny edge algorithm[13] and was insensitive to noise, easy to distinguish fake edges from real edges and more accurate to identify the IPFP boundary. The points at which image intensity changed sharply were typically organized into a set of curved line segments termed edges[14]. Base on this definition, the improved algorithm[13] scanned the groups of surrounding weak edges which were marked as adjacent to determine whether they should join into the strong edges or not. At last, an initial lasso which was created manually by a set of points in sequence near the outer contour of IPFP would begin to contract inward to find the real edge.

The regions in IPFP with high intensity were obtained subsequently. Because the pixels in the high intensity region had similar signal intensity, the new algorithm, which was based on the region growing algorithm[15], was developed. It was robust, rapid, automatic, and free of manual parameter-tuning for segmentation of the high intensity region in IPFP. This was an approach to examine neighbouring pixels of initial seed points and to determine whether the pixel neighbours should be added to the region. The algorithm was described as follows.

First, a set of seed points in IPFP, $P = \{P_1, P_2, \cdots, P_n\}$, was selected. We chose a set of regional maximum points of IPFP *via* 8-connected neighbourhoods[16]: $A = \{A_1, A_2, \cdots, A_k\}$, and then examined the histogram. The seed point was defined when its intensity was above threshold I_{th} calculated using Otsu' method[17]. That was, if $I_{A_i} > I_{th}$, point A_i was selected as a seed point, where "I" was the intensity value of the pixel. The initial region began with the exact location of these seeds.

Second, regions from the seed points were grown using 8-connected neighbourhood. We compared the intensity between neighbouring pixels and seed points. If the difference was less than "similarity threshold value", the neighbouring pixels were classified into the seed points. Similarity threshold value ε_j was defined as five percent of mean intensity of seed group P_j, $j = \{1, 2, \cdots, n\}$. If $\left|I_{N(P_j)} - \overline{I(P_j)}\right| < \varepsilon_j$, $N(P_j)$ was added to form the growing seed group P_j. $\overline{I(P_j)}$ was the mean value of P_j, and $N(P_j)$ was one of neighbouring pixels of P_j. This step was repeated until all $N(P_j)$ were classified. There was an iterative process until there was no change in seed group P_j between two successive steps. Then n of similar high intensity regions $\{P_1, P_2, \cdots, P_n\}$ were classified [Fig. 1(b)].

Measurements of high signal intensity in IPFP

Generally, the signal intensity of IPFP was not uniform in older adults or in patients with OA [Fig. 1(b) and (c)], so mean value of IPFP signal intensity [Mean (IPFP)] and standard deviation of IPFP signal intensity [sDev (IPFP)] was introduced to represent signal intensity variation of IPFP. The median value [Median (H)] and upper quartile value [UQ (H)] of the high signal intensity were used to represent the measures of high signal intensity. The volume of high signal intensity regions of IPFP [Volume (H)] was calculated according to the slice thickness and the area on each slice (Fig. 1), and the ratio of Volume (H) to volume of whole IPFP [Percentage (H)] was used to represent the adjusted quantity of these regions.

The clustering regions with high signal intensity in IPFP differed in different patients, which may have different clinical significance. Clustering factor (H) was therefore introduced to represent this clustering effect (Fig. 1). Calculation of clustering factor (H) was described as follows.

$$Clustering\ factor_{(H)} = \frac{\sum_{i=1}^{m} Vol_i / \sum_{j=1}^{n} Vol_j}{m/n}$$

Where,

$$m = \begin{cases} n*10\% & n > 10 \\ 1 & n \le 10 \end{cases}$$

n is the number of high intensity regions. Vol_j is the volume of seed group P_j. $\sum_{j=1}^{n} Vol_j$ is the total volume of high intensity regions.

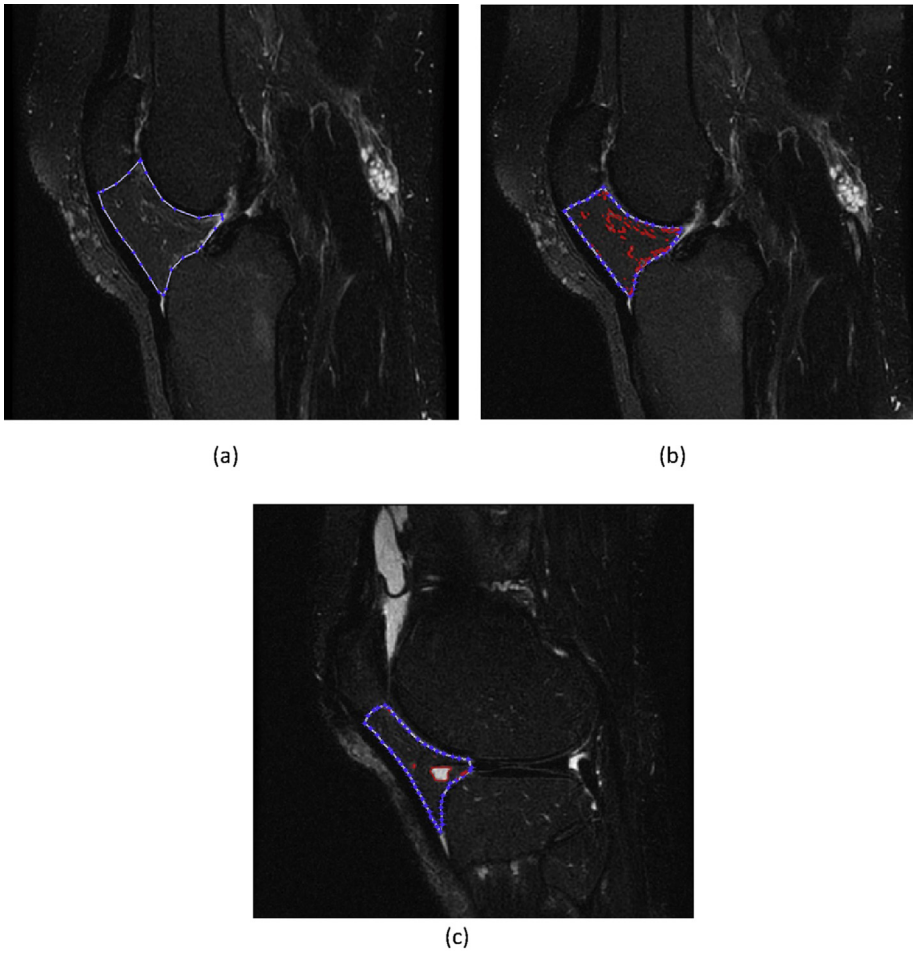

Fig. 1. Segmentation and intensity calculation of IPFP **on sagittal planes of fat-saturated T2-weighted images using MATLAB**. (a) The segmentation of IPFP is performed first. An initial lasso is created by a set of points near the outer contour of IPFP and then contracts inward to approximate the real boundary of IPFP automatically. (b) The red areas within the IPFP represent the high signal regions which are obtained by newly developed algorithm. The regions with high signal intensity scatter over whole IPFP. The total volume of these regions is 2.07 and clustering factor (H) is 5.15. (c) The sagittal slice of T2-weighted MRI shows regions with clustering high signal intensity. The total volume of these regions is 2.06 and clustering factor (H) is 7.51.

$\sum_{i=1}^{m} Vol_i$ is the volume of the top m largest high intensity regions. *Clustering factor*$_{(H)}$ reflects the actual clustering effects, the bigger the *Factor*$_{(H)}$, the greater the clustering effects. When we calculated m, we performed a validation analysis using 5%, 10%, 15%, 20% and 25% cut off values of n and found that 10–20% values were most significantly associated with outcome measures. 10% value was selected because it could catch small numbers of largest high intensity regions out of all high intensity regions (e.g., one largest high intensity region out of 10 high intensity regions).

A semi-quantitative method which we used previously[7] was utilized to re-assess high signal intensity within IPFP. The measurements were performed using sagittal planes of fat-saturated T2-weighted images and the signal alteration was graded as follows: grade 0 = none; grade 1 $\leq$ 10% of the region; grade 2 = 10–20% of the region; grade 3 $\geq$ 20% of the region. Intra-observer and interobserver reliabilities for the semi-quantitative method were assessed in 100 participants with an intraclass correlation coefficient (ICCs) of 0.90 and an interclass correlation coefficient of 0.89[7].

Measures for knee structural changes

In order to assess construct validity, we compared the IPFP measures with measures for knee structural changes, including cartilage defects, bone marrow lesions (BML) and ROA scores. Cartilage defects (0–4) were graded on T2-weighted images using a modified Outerbridge classification[18] at medial tibial, medial femoral, lateral tibial and lateral femoral sites. A total score was calculated as the sum of subregional scores. Intra-observer reliability ranged from 0.77 to 0.94.

BMLs were defined as discrete areas of increased signal adjacent to the subcortical bone, measured using modified Whole-Organ Magnetic Resonance Imaging Score (WORMS)[19] (0 = none; 1 $\leq$ 25% of the subregion; 2 = 25–50%; 3 $\geq$ 50%). A total score was calculated as the sum of subregional scores. The ICCs were 0.93–0.98 for this scoring system.

A standing anteroposterior X-ray of the symptomatic knee with 15° flexion was applied for each participant. JSN and osteophytes were assessed individually on the film on a scale of 0–3 (0 = normal and 3 = most severe) according to the Osteoarthritis Research Society International (OARSI) atlas developed by Altman *et al.*[11]. We summed the osteophyte and JSN scores as the knee total ROA score, as previously described[20].

Statistical analysis

Reliability

To calculate intra-reader and inter-reader reliabilities, signal intensity measures were repeated by one reader (1 month later) or

scored by two readers independently in 50 randomly selected participants. ICC and interclass correlation coefficients were calculated.

Concurrent validity

High signal intensity was measured by quantitative and semi-quantitative methods, and the concurrent validity of each quantitative measure was tested with the semi-quantitative measurement using a non-parametric (Spearman's) correlation analysis.

Clinical construct validity

Clinical construct validity was examined by carrying out both linear regressions and ordinal logistic regressions to examine the associations between IPFP signal intensity measures including Mean (IPFP), sDev (IPFP), Median (H), UQ (H), Volume (H), Percentage (H) as well as Clustering factor (H) (independent variables) and dependent variables (cartilage defects, BMLs, and ROA scores) before and after adjustment for age, sex and body mass index (BMI). For ordinal logistic regressions, dependent variables were stratified into four groups according to quartile values (1–4).

Results

Subject characteristics

A total of 100 participants (women: 45%, mean age: 63.9 years ranging from 51 to 79 years) were included in the present study. Baseline characteristics of the participants were presented in Table I.

Reliability

The ICCs for intra- and inter-observer correlation coefficients of IPFP signal intensity measurements are presented in Table II. The ICCs and inter-observer correlation coefficients for all measures are high (>0.90). Only 1 min was required for the segmentation, placement of seed points, necessary corrections, calculation and data output for each participant.

Table I
Baseline characteristics of participants ($n = 100$)

Characteristic	Values*
Age (years)	63.9 (6.8)
Female sex (%)	45
Height (cm)	169.9 (9.6)
Weight (kg)	85.7 (15.0)
BMI (kg/m^2)	29.7 (4.7)
TF cartilage defects scores	14.0 (4.1)
TF BML scores	4.1 (3.8)
Total ROA scores	7.9 (5.1)
Mean (IPFP)	0.2 (0.03)
sDev (IPFP)	0.1 (0.02)
Median (H)	0.3 (0.05)
UQ (H)	0.4 (0.1)
Volume (H)	2.0 (0.6)
Percentage (H)	0.1 (0.01)
Clustering factor (H)	6.0 (0.7)

* Mean (SD) or percentage of patients. BMI, body mass index; BML, bone marrow lesion; ROA, radiographic osteoarthritis; IPFP: infrapatellar fat pad; TF, tibiofemoral; Mean (IPFP), mean value of IPFP intensity; sDev (IPFP), standard deviation of IPFP signal intensity; Median (H), median value of high signal intensity region; UQ (H), upper quartile value of high signal intensity region; Volume (H), volume of high signal intensity region; Percentage (H): ratio of volume of high signal intensity region/whole IPFP volume; Clustering factor (H): clustering factor of high signal intensity.

Table II
Intra- and inter-observer correlation coefficients for IPFP measurements

	Intra-observer	Inter-observer
Mean (IPFP)	0.99	1.00
sDev (IPFP)	0.97	0.90
Median (H)	0.95	0.99
UQ (H)	0.98	0.91
Volume (H)	0.99	0.99
Percentage (H)	0.95	0.96
Clustering factor (H)	0.96	0.93

IPFP: infrapatellar fat pad; Mean (IPFP), mean value of IPFP intensity; sDev (IPFP), standard deviation of IPFP signal intensity; Median (H), median value of high signal intensity region; UQ (H), upper quartile value of high signal intensity region; Volume (H), volume of high signal intensity region; Percentage (H): ratio of volume of high signal intensity region/whole IPFP volume; Clustering factor (H): clustering factor of high signal intensity.

Concurrent validity

Significant correlations were found between the semi-quantitative score and quantitative measures [$r = 0.30$ and 95% CI: 0.15–0.44 for Mean (IPFP), $r = 0.74$ and 95% CI: 0.66–0.80 for sDev (IPFP), $r = 0.58$ and 95% CI: 0.46–0.67 for Median (H), $r = 0.60$ and 95% CI: 0.49–0.69 for UQ (H), $r = 0.19$ and 95% CI: 0.04–0.34 for Volume (H), $r = 0.37$ and 95% CI: 0.22–0.49 for Percentage (H) and $r = 0.49$ and 95% CI: 0.39–0.58 for Clustering factor (H); all $P < 0.001$].

Clinical construct validity

Table III described the associations between IPFP measurements and cartilage defects. In both linear regression and ordinal logistical regression analyses, sDev (IPFP), Volume (H), Percentage (H) and Clustering factor (H) were significantly and positively associated with tibiofemoral (TF) cartilage defects before and after adjustment for age sex and BMI. Median (H) and UQ (H) were significantly associated with quartiles of TF cartilage defect score before and after adjustment for age sex and BMI. In contrast, Mean (IPFP) was not significantly associated with cartilage defects at any site.

Table IV described the associations between IPFP measurements and TF BMLs. In both linear regression and ordinal logistical regression, sDev (IPFP) and Clustering factor (H) were significantly and positively associated with TF BMLs before and after adjustment for age sex and BMI. In contrast, other IPFP measurements were not significantly associated with TF BMLs before and after adjustment.

Table V described the associations between IPFP measurements and ROA. In both linear regression and ordinal regression, four IPFP measurements except for Mean (IPFP), Median (H) and UQ (H) were positively and significantly associated with ROA scores before and/or after adjustment for age, sex and BMI.

The semi-quantitative score of IPFP signal intensity alteration was only significantly associated with TF cartilage defects, but not with BMLs and ROA before and after adjustment for age, sex and BMI (data not shown).

Discussion

This study demonstrates a novel quantitative method measuring signal intensity of IPFP which provides continuous variables that may be sensitive to the changes. Evidence of concurrent validity was proven through a non-parametric correlation analysis between two measurements (quantitative and semi-

Table III
Associations between IPFP measurements and TF cartilage defects

	Univariable	Multivariable*
Total cartilage defect score	***β (95% CI)***	***β (95% CI)***
Mean (IPFP)	0.01 (−22.93, 24.87)	0.02 (−23.49, 27.44)
sDev (IPFP)	**0.35 (0.01, 0.70)**	**0.38 (0.01, 0.76)**
Median (H)	0.14 (−3.73, 20.40)	0.15 (−3.90, 21.50)
UQ (H)	0.57 (−0.35, 1.49)	0.60 (−0.37, 1.58)
Volume (H)	**0.30 (0.53, 2.56)**	**0.44 (1.00, 3.66)**
Percentage (H)	**0.74 (0.28, 1.21)**	**0.73 (0.26, 1.20)**
Clustering factor (H)	**1.69 (0.88, 2.50)**	**1.67 (0.85, 2.50)**
Total cartilage defect score quartiles	***OR (95% CI)***	***OR (95% CI)***
Mean (IPFP) (per 10 unit)	1.65 (0.41, 6.67)	1.77 (0.41, 7.69)
sDev (IPFP) (per 100 unit)	**1.37(1.10, 1.71)**	**1.46 (1.15, 1.86)**
Median (H) (per 10 unit)	**2.31(1.11, 4.81)**	**2.61(1.21, 5.64)**
UQ (H) (per 10 unit)	**1.84 (1.05, 3.22)**	**2.03(1.13, 3.67)**
Volume (H)	**2.59 (1.35, 4.96)**	**5.26 (2.13, 12.97)**
Percentage (H) (per 100 unit)	**1.58(1.16, 2.14)**	**1.57(1.16, 2.13)**
Clustering factor (H)	**3.19(1.80, 5.66)**	**3.22(1.81, 5.75)**

* Adjusted for age, sex and BMI. TF, tibiofemoral; IPFP: infrapatellar fat pad; Mean (IPFP), mean value of IPFP intensity; sDev (IPFP), standard deviation of IPFP signal intensity; Median (H), median value of high signal intensity region; UQ (H), upper quartile value of high signal intensity region; Volume (H), volume of high signal intensity region; Percentage (H): ratio of volume of high signal intensity region/whole IPFP volume; Clustering factor (H): clustering factor of high signal intensity. Significant differences are shown in bold.

Table IV
Associations between IPFP measurements and TF BMLs

	Univariable	Multivariable*
Total bone marrow lesion score	***β (95% CI)***	***β (95% CI)***
Mean (IPFP)	0.01 (−26.76, 28.44)	0.01 (−28.16, 30.21)
sDev (IPFP)	**0.44 (0.08, 0.80)**	**0.42 (0.03, 0.81)**
Median (H)	0.19 (−0.34, 27.26)	0.18 (−2.06, 26.90)
UQ (H)	0.87 (−0.08, 1.83)	0.81 (−0.21, 1.82)
Volume (H)	0.19 (−0.03, 2.36)	0.20 (−0.41, 2.78)
Percentage (H)	0.48 (−0.02, 0.98)	0.50 (−0.01, 1.01)
Clustering factor (H)	**1.73 (0.88, 2.58)**	**1.73 (0.86, 2.60)**
Total bone marrow lesion score quartiles	***OR (95% CI)***	***OR (95% CI)***
Mean (IPFP) (per 10 unit)	0.82 (0.21, 3.30)	0.87 (0.20, 3.77)
sDev (IPFP) (per 100 unit)	**1.27 (1.03, 1.57)**	**1.27(1.01, 1.59)**
Median (H) (per 10 unit)	1.70 (0.83, 3.48)	1.70 (0.81, 3.59)
UQ (H) (per 10 unit)	1.55 (0.90, 2.68)	1.53 (0.86, 2.71)
Volume (H)	1.72 (0.92, 3.22)	1.96 (0.86, 4.47)
Percentage (H) (per 100 unit)	1.30 (0.97, 1.73)	1.32 (0.97, 1.73)
Clustering factor (H)	**2.78(1.60, 4.85)**	**2.85(1.62, 5.00)**

* Adjusted for age, sex and BMI. BMI, body mass index; TF, tibiofemoral; IPFP: infrapatellar fat pad; Mean (IPFP), mean value of IPFP intensity; sDev (IPFP), standard deviation of IPFP signal intensity; Median (H), median value of high signal intensity region; UQ (H), upper quartile value of high signal intensity region; Volume (H), volume of high signal intensity region; Percentage (H): ratio of volume of high signal intensity region/whole IPFP volume; Clustering factor (H): clustering factor of high signal intensity. Significant differences are shown in bold.

quantitative) of IPFP and the clinical construct validity was demonstrated by showing significant associations of quantitative IPFP intensity measurements with knee joint structural changes (cartilage defects, BMLs and ROA). Meanwhile, tests of the intra-observer and inter-observer reliabilities showed that quantitative IPFP measurements were highly reproducible.

Knee OA is considered as a whole joint disease involving all elements in the knee joints including IPFP which is regarded as an emerging player in the onset and progression of knee OA. Several studies[5,6] have been conducted in this area trying to find the relationships between IPFP size and the changes of knee structures or symptoms. Increased signal intensity within IPFP on T2-weighted MR images may represent some pathological changes such as inflammation and oedema[3,4]. In view of the concept that knee OA is a whole joint disease, it is reasonable to generate a hypothesis that signal intensity changes of IPFP on MR image are associated with osteoarthritic changes in the knee joint.

Recently we reported that IPFP signal intensity changes assessed semi-quantitatively were associated with clinical and structural abnormalities of knee joints in old adults cross-sectionally and longitudinally[7]. However, this semi-quantitative scale may be less sensitive than quantitative measurements for changes over time. The cost can be high due to the expense for radiology expertise and long time required for reading of IPFP slice by slice. Furthermore, it also needs a subjective decision while scoring the intensity change, making it less reproducible than quantitative measurements.

To date, there have been few reports using quantitative approaches to assess IPFP signal intensity[9]. In our study, the algorithm was well designed to segment IPFP semi-automatically and to obtain the high signal intensity regions automatically. Four categories (signal intensity of whole IPFP, high signal intensity of IPFP, volume of high signal intensity and clustering effect of high signal intensity) and seven measurements of IPFP intensity, which represented the extent and the clustering effect, were calculated automatically for each subject. The algorithm was based on the inherently digital nature of MR images and was well programmed to segment the IPFP and calculate the intensity, so the new method, is obviously more accurate and efficient. It can provide quantitative scores which should be more sensitive to the change in longitudinal studies. Furthermore, it could be cost saving because radiology

Table V
Associations between IPFP measurements and ROA score

	Univariable	Multivariable*
Total ROA score	***β (95% CI)***	***β (95% CI)***
Mean (IPFP)	0.04 (−40.83, 59.50)	0.09 (−30.08, 69.69)
sDev (IPFP)	**0.76 (0.09, 1.43)**	**0.76 (0.05, 1.47)**
Median (H)	0.17 (−6.02, 41.74)	0.18 (−5.60, 42.72)
UQ (H)	1.31 (−0.50, 3.11)	1.35 (−0.53, 3.22)
Volume (H)	**0.36(1.22, 5.05)**	**0.41(1.10, 6.19)**
Percentage (H)	**1.38 (0.36, 2.39)**	**1.18 (0.15, 2.21)**
Clustering factor (H)	**2.28 (0.42, 4.13)**	1.82 (−0.08, 3.72)
Total ROA score quartiles	***OR (95% CI)***	***OR (95% CI)***
Mean (IPFP) (per 10 unit)	1.13 (0.21, 6.19)	1.78 (0.30, 10.65)
sDev (IPFP) (per 100 unit)	**1.36(1.05, 1.75)**	**1.40 (1.05, 1.87)**
Median (H) (per 10 unit)	1.77 (0.77, 4.08)	1.95 (0.79, 4.83)
UQ (H) (per 10 unit)	1.53 (0.81, 2.88)	1.63 (0.80, 3.32)
Volume (H)	**4.38(1.95, 9.81)**	**6.75(2.18, 20.87)**
Percentage (H) (per 100 unit)	**1.81(1.22, 2.68)**	**1.77 (1.18, 2.67)**
Clustering factor (H)	**2.57 (1.28, 5.15)**	**2.25 (1.08, 4.66)**

* Adjusted for age, sex and BMI. BMI, body mass index; ROA: radiographic osteoarthritis; IPFP: infrapatellar fat pad; Mean (IPFP), mean value of IPFP intensity; sDev (IPFP), standard deviation of IPFP signal intensity; Median (H), median value of high signal intensity region; UQ (H), upper quartile value of high signal intensity region; Volume (H), volume of high signal intensity region; Percentage (H): ratio of volume of high signal intensity region/whole IPFP volume; Clustering factor (H): clustering factor of high signal intensity. Significant differences are shown in bold.

expertise is not required in the reading process but the knowledge of anatomy, pathology and radiological principles is preferred to operate the software.

To confirm clinical construct validity, each measure of IPFP intensity was tested for its association with ROA, cartilage defects and BMLs by linear regressions and ordinal logistic regression. Obviously, the clinical construct validity was established by attaining significant associations of most measurements of IPFP intensity with joint structural abnormalities. Among these measurements, Clustering factor (H) and sDev (IPFP) were consistently and significantly associated with all joint structural measurements, indicating that Clustering factor (H) and sDev (IPFP), which reflect the clustering effect of high signal intensity region and signal intensity heterogeneity within IPFP, respectively, have greater construct validity. In both linear regression and ordinal regression, Percentage (H) and Volume (H) were consistently and significantly associated with knee cartilage defects and ROA but not with BMLs, while Median (H) and UQ (H) were only significantly associated with TF cartilage defects in ordinal regression. Therefore, IPFP measurements of Volume (H), Percentage (H), Median (H) and UQ (H) may also be valid but need to be further investigated. In contrast, Mean (IPFP) was not significantly associated with any knee structural measurements, suggesting that simple measurement of mean signal intensity in IPFP may not have clinical construct validity.

The main strength of this study included blind readings, the standardized methods used for data acquisition and high intra- and inter-reader reliabilities. The semi-automatic algorithm was able to find the real edge of IPFP accurately and high signal intensity regions were obtained simultaneously. Manual corrections for the IPFP boundaries were needed for a few cases. This study had several potential limitations. First, MR images were obtained using a 1.5-T whole body MRI unit with fat-saturated T2-weighted FSE sequence which provided excellent visualization of IFPF. However, we did not examine signal intensity of IPFP using other MRI sequences, which may have a different performance. Second, the low intensity regions within IPFP frequently coexisted with high signal intensity regions, which were not taken into account by this method. Low signal intensity in IPFP may be associated with clinical and structural outcomes in knee OA, so further modification to include these low intensity regions would be done. Last, the cross-sectional nature of this study precluded any inference about predictive validity. Longitudinal studies were needed to address the causality.

Conclusions

A novel and efficient method to segment IPFP and calculate its signal intensity on T2-weighted MRI images is documented. This method is reproducible, and has concurrent and clinical construct validity, but its predictive validity needs to be examined by future longitudinal studies.

Author contributions

CD had full access to all of the data in the study and took responsibility for the integrity of the data and the accuracy of the data analysis. CD carried out the study design, participated in the acquisition, analysis and interpretation of data, manuscript preparation, and statistical analysis. ML participated in the analysis and interpretation of data, manuscript preparation, and statistical analysis. ZC participated in the development of the new algorithm, acquisition and interpretation of data, statistical analysis, and manuscript preparation. WH participated in the acquisition and interpretation of data, statistical analysis, and manuscript preparation. ZZ participated in the acquisition and interpretation of data, and manuscript preparation. XJ participated in the acquisition and interpretation of data, and manuscript preparation. DH participated in the study design and manuscript preparation.

Conflict of interest

The authors declare that they have no conflict of interest.

Acknowledgements

J. Barling, K. Nguo, J. Hankin and A. Noone have been involved in the coordination of VIDEO study. G. Jones, F. Cicuttini, A. Wluka and T. Winzenberg were chief investigators of VIDEO study. CD is the recipient of an Australian Research Council Future Fellowship. DH is the recipient of a Practitioner Fellowship from Australian National Health & Medical Research Council (NHMRC). This study was supported by NHMRC (Project Grant Code 605501).

References

1. Hunter DJ, Felson DT. Osteoarthritis. BMJ (Clinical Res ed.) 2006;332(7542):639–42.
2. Poole AR. Osteoarthritis as a whole joint disease. HSS J Musculoskelet J Hosp Special Surg 2012;8(1):4–6.
3. Ioan-Facsinay A, Kloppenburg M. An emerging player in knee osteoarthritis: the infrapatellar fat pad. Arthritis Res Ther 2013;15(6):225.
4. Jacobson JA, Lenchik L, Ruhoy MK, Schweitzer ME, Resnick D. MR imaging of the infrapatellar fat pad of Hoffa. Radiographics 1997;17(3):675–91.
5. Han W, Cai S, Liu Z, Jin X, Wang X, Antony B, *et al.* Infrapatellar fat pad in the knee: is local fat good or bad for knee osteoarthritis? Arthritis Res Ther 2014;16(4):R145.
6. Cowan SM, Hart HF, Warden SJ, Crossley KM. Infrapatellar fat pad volume is greater in individuals with patellofemoral joint osteoarthritis and associated with pain. Rheumatol Int 2015;35(8):1439–42.
7. Han W, Aitken D, Zhu Z, Halliday A, Wang X, Antony B, *et al.* Signal intensity alteration in the infrapatellar fat pad at baseline for the prediction of knee symptoms and structure in older adults: a cohort study. Ann Rheum Dis 2015.

8. Atukorala I, Kwoh CK, Guermazi A, Roemer FW, Boudreau RM, Hannon MJ, *et al*. Synovitis in knee osteoarthritis: a precursor of disease? Ann Rheum Dis 2016;75(2):390–5.
9. Eckstein F, Diepold J, Ruhdorfer A, Dannhauer T, Wirth W, Guermazi A. Infra-patellar fat pad morphology and MRI signal distribution in advanced radiographic knee OA – data from the OAI. Osteoarthritis Cartilage 2015;23:A219.
10. Altman R, Asch E, Bloch D, Bole G, Borenstein D, Brandt K, *et al*. Development of criteria for the classification and reporting of osteoarthritis. Classification of osteoarthritis of the knee. Diagnostic and Therapeutic Criteria Committee of the American Rheumatism Association. Arthritis Rheum 1986;29(8):1039–49.
11. Altman RD, Gold GE. Atlas of individual radiographic features in osteoarthritis, revised. Osteoarthritis Cartilage/OARS, Osteoarthr Res Soc 2007;15(Suppl A):A1–A56.
12. Cao Y, Jones G, Cicuttini F, Winzenberg T, Wluka A, Sharman J, *et al*. Vitamin D supplementation in the management of knee osteoarthritis: study protocol for a randomized controlled trial. Trials 2012;13:131.
13. Geng X, Chen K, Hu XG. An improved Canny edge detection algorithm for color image. IEEE Intl Conf Ind Inform 2012:113–7.
14. Canny J. A computational approach to edge detection. IEEE Trans Pattern Analysis Mach Intell 1986;8(6):679–98.
15. Adams R, Bischof L. Seeded region growing. IEEE Trans Pattern Analysis Mach Intell 1994;16(6):641–7.
16. Cheng CC, Peng GJ, Hwang WL. Subband weighting with pixel connectivity for 3-D wavelet coding. IEEE Trans Image Process 2009;18(1):52–62.
17. Otsu N. Threshold selection method from gray-level histograms. IEEE Trans Syst Man Cybern 1979;9(1):62–6.
18. Baysal O, Baysal T, Alkan A, Altay Z, Yologlu S. Comparison of MRI graded cartilage and MRI based volume measurement in knee osteoarthritis. Swiss Med Wkly 2004;134(19–20):283–8.
19. Peterfy CG, Guermazi A, Zaim S, Tirman PF, Miaux Y, White D, *et al*. Whole-organ Magnetic Resonance Imaging Score (WORMS) of the knee in osteoarthritis. Osteoarthritis Cartilage/OARS, Osteoarthr Res Soc 2004;12(3):177–90.
20. Jones G, Ding C, Scott F, Glisson M, Cicuttini F. Early radiographic osteoarthritis is associated with substantial changes in cartilage volume and tibial bone surface area in both males and females. Osteoarthritis Cartilage/OARS, Osteoarthr Res Soc 2004;12(2):169–74.